

Influence of solar variability on the occurrence of Central European weather types from 1763 to 2009

Mikhaël Schwander^{1,2}, Marco Rohrer^{1,2}, Stefan Brönnimann^{1,2}, Abdul Malik^{1,2}

¹Institute of Geography, University of Bern, Bern, 3012, Switzerland

5 ²Oeschger Centre for Climate Change Research, University of Bern, Bern, 3012, Switzerland

Correspondence to: Mikhaël Schwander (mikhael.schwander@giub.unibe.ch)

Abstract. The impact of solar variability on weather and climate in Central Europe is still not well understood. In this paper we use a new time series of daily weather types to analyse the influence of the 11-year solar cycle on the tropospheric weather of Central Europe. We employ a novel, daily weather type classification over the period 1763-2009 and investigate the occurrence frequency of weather types under low, moderate and high solar activity level. Results show a tendency towards fewer days with westerly and west south-westerly flow over Central Europe under low solar activity. In parallel, the occurrence of northerly and easterly types increases. For the 1958-2009 period, a more detailed view can be gained from reanalysis data. Mean sea level pressure composites under low solar activity also show a reduced zonal flow, with an increase of the mean blocking frequency between Iceland and Scandinavia. Weather types and reanalysis data show that the 11-year solar cycle influences the late winter atmospheric circulation over Central Europe with colder (warmer) conditions under low (high) solar activity. Model simulations used for a comparison do not reproduce the imprint of the 11-year solar cycle found in the reanalyses data.

1. Introduction

The effects of solar activity changes on weather and climate in Europe are still not well understood. Although there is both empirical and model evidence of an imprint of the 11-yr sunspot cycle in the stratosphere, climate effects at the Earth's surface are less clear, nor are the mechanisms understood. Considering the rather small changes in the incoming energy over an 11-yr sunspot cycle of ca. 0.1% (and perhaps also over longer periods), many of the suggested mechanisms are indirect and involve changes in atmospheric circulation (Gray et al. 2010; Seppälä et al. 2014, for a review). Therefore, analysing changes in atmospheric circulation with regard to the 11-yr sunspot cycle might help to better attribute climatic changes to solar forcing. In this paper we analyse the imprint in atmospheric circulation.

Solar activity can have effects on the atmospheric circulation through three different mechanisms. These effects may arise from direct changes in total solar irradiance (TSI), from changes in stratospheric ozone and heating induced by changes in solar UV, or from changes in stratospheric ozone induced by energetic particles, whose flux is modulated by solar activity. The $\sim 1 \text{ Wm}^{-2}$ variation in TSI over an 11-yr sunspot cycle corresponds to a change in the radiation forcing of about ~ 0.17

Wm⁻² (Haigh 2003; Gray et al., 2010). This change in radiation forcing is estimated to cause a change in Earth's surface temperature of approximately 0.07 K and - with a lagged response - to changes in sea-surface temperatures (SSTs) (Gray et al., 2010; Stevens and North, 1996; White et al., 1997). Circulation effects (bottom-up mechanism) may arise from unequal heating or ocean feedbacks that might involve the North Atlantic (Thiéblemont et al., 2015). The increased UV radiation during sunspot maxima leads directly to an ozone increase and associated heating in the upper stratosphere (~40 km) (e.g., Matthes et al., 2004; Sitnov, 2009) and to changes in tropospheric circulation via downward propagation from the stratosphere (top-down mechanism). The suspected effects project strongly onto the North Atlantic European sector (Baldwin et al. 2001). The energetic particle flux (proton and electron), which is peaking in the declining phase of the sunspot cycle, leads to the production of NO_x in the mesosphere and stratosphere, which can destroy ozone in the stratosphere (Andersson et al., 2014; Päivärinta et al., 2013; Solomon et al., 1982). Through downward propagation, the troposphere can be affected, but a short phase lag is expected. Rozanov et al. (2012) showed that precipitating energetic particles can influence the chemical composition of the atmosphere as well as its dynamic down to the troposphere. The mechanisms might lead to different temporal (i.e., lagged or not) or spatial circulation changes, hence it is important to well characterise the circulation response of the 11-year solar cycle.

For all of the mechanisms, the response is expected to be pronounced over the North Atlantic European sector. In fact, many observation-based studies have found effects of the 11-year sunspot cycle in European weather and climate (e.g., Barriopedro et al., 2008; Brugnara et al., 2013; Huth et al., 2007; Ineson et al., 2011; Lockwood et al., 2010; Van Loon and Meehl, 2014). The impact of solar activity on variability modes such as the Atlantic Oscillation (AO) or the North Atlantic oscillation (NAO) is often investigated. The AO - which is correlated with the NAO - was shown to be influenced in his intensity and variability by the 11-year solar cycle (Huth et al., 2007). The NAO was found to be linked to the 11-year cycle with a positive (negative) pattern being associated to high (low) solar activity (e.g., Gimeno et al., 2003; Ineson et al., 2011; Lockwood, 2012; Sfca et al., 2015; Woollings et al., 2010). Ineson et al. (2011) found a response to low solar activity in models which is similar to the negative NAO pattern. A similar pattern under low solar activity was found by Woollings et al. (2010). Brugnara et al. (2013) did not find a significant correlation between the solar activity and the NAO, although they found a reduced westerly flow over the North Atlantic under low solar activity. (Van Loon and Meehl, 2014) found that the NAO is enhanced when in phase with solar maxima, as when it is out of phase the NAO is negative. Thiéblemont et al. (2015) found that the solar activity influence project onto the NAO with the strongest signal visible with a 3-year lag. A similar lag was also found in Gray et al. (2013). Scaife et al. (2013) proposed a mechanism to explain this lag through the direct response to solar UV irradiance change and the effect of the Atlantic SST on the NAO. The link between solar activity and the NAO is not supported by all studies. van Oldenborgh et al. (2013) found no statistically significant linear relation between the sunspot number and the NAO.

The North Atlantic circulation shows a response to the 11-year cycle, which leads to changes in the European weather that could only be visible on short time-scales. Atmospheric circulation over Europe is strongly correlated to the NAO and hence

solar activity is thought to have an influence on weather conditions in Europe in winter. Studies show a preference of cold winters in Europe to be associated with minima in the 11-year solar cycle (e.g., Lockwood et al., 2010; Sirocko et al., 2012). Changes in the atmospheric circulation over the North Atlantic linked to solar activity might have an impact on European weather on short time-scale. For example Barriopedro et al. (2008) analysed the duration in days of blockings linked to solar activity. They found that North Atlantic blocking persistence increases under low solar activity and they are positioned more to the east.

Model simulations have also been used to investigate the solar activity impact on climate (see Gray et al., 2010 for a review). Uncertainties are however still large concerning the response in the troposphere. Models can reproduce the main influence of the solar activity on the troposphere but some of them have difficulties to reproduce details. For instance, Gray et al. (2013) found a lag in the solar response over Europe and the North Atlantic in observation data which was not confirmed by model simulations. Gray et al. (2013) also concluded that there is no consensus between climate models on the influence of the 11-year solar cycle and the linked mechanisms. Matthes et al. (2003) compared the response of several global circulation models to the 11-year solar signal over Europe and the North Atlantic. One of their conclusions was that the late winter dynamical response in the model is not comparable to observations. More recently the solar signal was analysed in CMIP-5 simulations (Hood et al., 2015; Misios et al., 2016; Mitchell et al., 2015). For instance Mitchell et al. (2015) found a lag in the North Atlantic surface response to the 11-year solar cycle in the models but weaker than in the observations. Not all models reproduce a similar response to the 11-year solar cycle in the stratosphere compared to observations, but some of them do reproduce an increase of the polar night jet under high solar activity (Misios et al., 2016).

Others studies looked at the impact of solar activity on climate at longer time-scales. Martin-Puertas et al. (2012) used lake sediments to analyse variations in wind strength and the ^{10}Be accumulation rate for solar activity from 3300 to 2000 years before present. They found windy conditions in Western Europe during late winter under a long period of low solar activity. Moffa-Sánchez et al. (2014) used foraminifer shells to reconstruct the sea surface temperature and salinity of the North Atlantic over the past millennium. They found a correlation between centennial-scale variations in hydrography and total solar irradiance. On a shorter time-scale, Sirocko et al. (2012) analysed the occurrence of cold winters in Europe back to 1780 using documentary data. Sirocko et al. (2012) found cold winters in Europe to be often linked to the low activity phase of the 11-year solar cycle. The time resolution of these studies covering a long period is coarse (centennial-scale) or in the case of Sirocko et al. (2012) the method shows some weaknesses as explained in van Oldenborgh et al. (2013).

In this study, we analyse the influence of the 11-year solar cycle on Central European weather types. The aim is to identify how the variations in the mean atmospheric circulation over Europe can be explained by changes in the occurrence of weather types. For this we apply a similar approach as Huth et al. (2008b) by looking at the occurrence of weather types over Central Europe. There is a large panel of weather type classifications (WTCs) available for Europe based on various methods and covering different periods (Huth et al., 2008a; Philipp et al., 2010, 2014). Here we use a unique data set of daily weather types covering the period 1763-2009 (Schwander et al., 2017) . It allows us for the first time to investigate the impact of the

11-year solar cycle on European climate with an analysis of weather statistics over almost 250 years. This analysis is performed by looking at changes in weather type occurrence as well as within-type changes. We complete this analysis by comparing changes in reanalyses data with model simulations.

This paper is structured as follow. The data and the methods used to analyse the solar activity influence on weather types, reanalysis data and model simulations are explained in Section 2. The results are presented in Section 3 and discussed in Section 4. We conclude this work in Section 5.

2. Data and Methods

For our analysis of the impact of 11-year solar cycle, we first computed the mean differences between low and high solar activity for the sea level pressure (slp), 500 hPa geopotential height (z500), 850 hPa temperature (t850) and blocking frequency for the period 1958-2009 for January to March (JFM). For this, we used the ERA-40 (from January 1958 to March 2002, Uppala et al., 2005) and ERA-Interim (from January 2003 to March 2009, Dee et al., 2011) reanalyses data set (same method as in Section 2.5) and the monthly sunspot number as a measure of solar activity (Section 2.1). A two-tailed Student's t test was used to determine the 95% probabilities that the low and high solar activity composites are from two different populations. Then we extended the analysis by using weather types (Section 2.2) with focus and the occurrence changes (Section 2.3) and within-type differences (Section 2.4). The method for the blocking frequency used in the differences composites is described in Section 2.5. Finally, the mean differences computed from reanalyses were compared with model simulations (Section 2.6).

2.1 Solar activity

The monthly sunspot number is used as a measure of the 11-year solar cycle (Fig. 1). It is the longest record of solar variability available; daily sunspots data are available starting from 1818 but monthly or yearly data go back to 1700. Sunspots correspond to zones of strong magnetic field; therefore, many visible sunspots are synonym of an active sun as the quiet sun is free of any spot. The sunspots time series captures well the 11-year solar cycle and can therefore be used as a proxy for quantifying solar activity. The sunspots data were retrieved from the Sunspot Index and Long-term Solar Observations (SILSO) and World Data Center for the production, preservation and dissemination of the international Sunspot Number website from the Royal Observatory of Belgium. We use the revised data series available since the 1st of July 2015.

2.2 Weather type classification

Weather types are used to determine if the circulation differences observed in reanalyses are only due to changes in the mean circulation or if they result from a change in the occurrences of weather patterns. Weather types are a summary of recurrent dynamical patterns over a specification region, in our case Central Europe and the Alpine Region. For this, we use the CAP7

(cluster analysis of principal components) WTC (Schwander et al., 2017). CAP7 is a daily time series of weather types representing the mean atmospheric circulation in the Alpine Region and Central Europe over the period 1763-2009. This classification is a reconstruction of the CAP9 classification used by the Federal Office of Meteorology and Climatology MeteoSwiss (Weusthoff, 2011). CAP9 starts in 1957 and is updated to the present. The weather types were computed with the ERA-40 and ERA-Interim reanalyses dataset. For CAP7, CAP9 was used as referenced from 1958 to 1998 and was reconstructed back to 1763 using early instrumental data from European weather stations. The classification was reduced to 7 types (hence CAP7) by combining similar, not well discriminated types. Although CAP9 was originally computed for the Alpine Region and contains a limited number of patterns, it – as well as CAP7 – captures the main circulation patterns over Europe and the North Atlantic. The 7 types with their names and abbreviations are presented in Table 1. The weather types can be used to analyse changes in the frequency of occurrences (between-type changes, Section 2.3) from 1763 to 2009 and to investigate changes in their composite (within-type changes, Section 2.4) with reanalysis data from 1958 to 2009. The mean frequency of occurrence of each type for JFM over the period 1763 to 2009 is shown in Fig. 2. The z500 and slp composites for 1958-2009 computed with ERA-40 (1958-2002) and ERA-Interim (2003-2009) for JFM are shown in Fig. 3. The classification contains three continental types (NE, E and N), two westerly types (WSW and W), one cyclonic type (WC), and one anticyclonic type (HP). CAP7 is the only objective times series of daily weather types which covers almost 250 years in Europe. It also covers a longer period than any existing reanalysis (from which weather types can also be computed). For more information on the method of reconstruction, see Schwander et al. (2017). The daily weather types CAP7 are completed with a probability value of each day being correctly classified (relative to the reference classification). Since CAP7 is a reconstruction and cannot be compared to any other WTC back to 1763, this probability value provides an indication on the reliability of the classification for each day. This allows us later to omit days with a probability lower than a certain threshold (e.g. 75%).

2.3 Weather type occurrences

The following method is similar to the procedure applied in Huth et al. (2008b) but the CAP7 dataset used here covers a longer period of time. A comparison with Huth et al. (2008b) can however be done over the second part of the 20th century. To capture the influence of the sun on weather patterns, changes in the frequency of occurrence of the CAP7 weather types relative to variations in solar activity are analysed. It was shown that the strongest influence of solar activity on the low troposphere is visible during the late winter months because of the delayed propagation of the signal from the stratosphere to the troposphere (Ineson et al., 2011). Thus, the weather type analysis as well as reanalyses and model simulations analyses are performed on months of JFM. The sunspot number data was first divided in three categories, low, moderate and high solar activity using the 33rd and 66th percentile as thresholds (see Fig. 1). This method assumes that all solar minima reach a similar low intensity as the number of sunspot cannot go below zero. The daily weather types were then classified to the corresponding solar activity level. For each weather type we computed the ratios of the frequency for each solar activity level (low, moderate, high) relative to the long-term mean. Results are calculated for the period January 1763 to March 2009

as well as for three sub-periods: 1763-1886, 1887-2009, and 1958-2009 (period of reanalysis data) for a comparison with Huth et al. (2008b). We removed 3 years following large volcanic eruptions as they can have a significant influence on climate (e.g., Robock, 2000). The three groups of solar activity are therefore of different sizes (see Table 2). The list of volcanic eruption was taken from Arfeuille et al. (2014). A resampling method was used to test the significance of the ratios

5 The weather type series (for each period) was resampled 10000 times. The computed ratio is considered as significant when below (above) the 250th (9750th) value of the resample elements. Another series of histogram (not shown) was computed using only days having a probability (to be correctly classified) superior to 75%. We also computed the ratios with a 1, 2 and 3-year lag for the 1763-2009 period.

2.4 Within-type differences

10 In addition to the change in the weather types occurrences, we investigate the within-type difference of atmospheric fields between low and high solar activity levels for each of the 7 weather types. For this, we computed composites for each weather type in order to identify changes in their mean circulation pattern over Europe and the North Atlantic under low and high solar activity. Composites of slp, z500 and t850 of each type were computed for the previously defined high and low solar activity classes for the period 1958-2009 (JFM). Additionally to these parameters, the mean blocking frequency was

15 also computed for each composite (see Section 2.5). From these composites, differences were calculated by subtracting the high activity from the low activity composites. ERA-40 (January 1958-March 2002) and ERA-Interim (January 2003-March 2009) were used as the original CAP types were computed based on the ERA-40 and ERA-Interim mean slp field. The reanalysis data were remapped to $1^\circ \times 1^\circ$ to be combined. The within-types analysis can therefore only be made over the period 1958-2009 and cannot be extrapolated back to 1763.

20 2.5 Blocking Frequency

Blockings are defined as reversal of the meridional geopotential height gradient at 500 hPa. We follow the approach of Tibaldi and Molteni (1990) and extended the blocking algorithm to find blockings in a two dimensional field following the procedure of Scherrer et al. (2006). The algorithm flags a certain longitude and latitude as blocked, if two criteria are fulfilled:

25

1. GPH gradient towards the pole

$$GPHG_P = Z500(\varphi + 14) - \frac{Z500(\varphi)}{\varphi + 14 - \varphi} < -10 \frac{\text{gpm}}{^\circ\text{lat}} \quad (1)$$

2. GPH gradient towards the equator

$$GPHG_E = Z500(\varphi) - \frac{Z500(\varphi - 14)}{\varphi - \varphi - 14} > 0 \frac{\text{gpm}}{^\circ\text{lat}} \quad (2)$$

30

The latitude φ varies from 36° to 76° in 2° intervals. ERA-40 data is bilinearly interpolated to a $2^\circ \times 2^\circ$ before computation.

Only blockings with a minimum lifetime of 5 days and spatial overlap larger than 70% between each time step are considered here.

2.6 Model simulations

In the last part of this paper we have employed the Coupled Atmosphere-Ocean-Chemistry Climate Model (AOCCM) simulations carried out with SOCOL-MPIOM (see, Muthers et al. 2014). The SOCOL (Solar Climate Ozone Links) chemistry-climate model is coupled to the ocean-sea-ice model MPIOM. The SOCOL is based on the middle atmosphere model MA-ECHAM5 version 5.4.01 (Roeckner et al., 2003) and a modified version of the chemistry model MEZON (Model for Evaluation of oZONe trends, Egorova et al., 2003). The model has a horizontal resolution of T31 ($3.75^\circ \times 3.75^\circ$) with 39 irregular vertical pressure levels (L39) from 1000 hPa to 0.01 hPa. The horizontal resolution of the ocean component (MPIOM) is 3° varying between Greenland (22 km) and tropical Pacific (350 km). The SOCOL-MPIOM cannot reproduce the Quasi-Biennial-Oscillation (QBO), thus nudged to QBO reconstruction from Brönniman et al. (2007). The MA-ECHAM5 (MPIOM) component calculates the dynamical processes in every 15 (144) minutes and atmosphere-ocean coupling takes place in every 24 hours (Anet et al. 2013a, b; Muthers et al. 2014). Muthers et al. 2014 employed SOCOL-MPIOM to carry out four transient simulations (namely L1, L2, M1, and M2) over the period AD 1600-1999 with all major forcings (i.e. greenhouse gases, volcanic eruptions, aerosols, and solar spectral irradiance), and interactive ozone chemistry. The SOCOL-MPIOM was forced with six bands of Solar Spectral Irradiance (SSI) reconstruction of Shapiro et al. (2011) over the Ultraviolet (UV), visible, and near infrared ranges. The L1 (M1) and L2 (M2) simulations were forced with large (small) mean solar amplitude of 6 (3) W/m² with different ocean initial conditions for both runs. For more details of the model the reader is referred to Muthers et al. 2014. The model is well capable of simulating the top-down (stratospheric-tropospheric coupling) and bottom-up (coupled ocean-atmosphere response) mechanisms as proposed by Meehl et al. (2009). For more information on the SOCOL-MPIOM model see Muthers et al. (2014).

We used the four model simulations (M1, M2, L1 and L2) and removed again 3 years following large volcanic eruptions (Arfeuille et al., 2014). The 11-year solar cycle was analysed similarly as for the weather types (33rd and 66th percentile thresholds of the sunspot number) since the sunspot number was used in the Shapiro et al. (2011) reconstruction. The period 1958-1999 was selected for comparison with the reanalysis data (1958-2009).. High and low solar activity composites were computed for slp and t850, and the low minus high activity difference was calculated. TSI forcing is correlated with the anthropogenic forcing (carbon dioxide - CO₂, methane - CH₄, nitrogen dioxide - N₂O and chlorofluorocarbons CFCs) with an increase over the 19th and 20th century. These anthropogenic forcings were taken from the PMIP3 database (Etheridge et al., 1996, 1998; Ferretti et al., 2005; MacFarling-Meure et al., 2006). Both forcings (solar and anthropogenic) reach their highest values at the end of the 20th century (see Muthers et al., 2014). We removed the anthropogenic forcing by applying a linear regression:

$$y_i = \alpha + \beta x_i + \varepsilon \quad (3)$$

where y is the predicted value and x the predictor (radiative forcing, CO₂, CH₄, N₂O and CFCs), α the intercept, β the regression coefficient and ε the residual.

3. Results

3.1 Mean difference

5 The differences computed between low and high solar activity with ERA-40 and ERA-Interim for 1958-2009 (Fig. 4) show a reduced zonal flow over Europe under low solar activity relative to high activity. The slp is higher between Iceland and Scandinavia, and lower over Southern Europe and the Mediterranean Sea. The z500 differences have a similar pattern but with higher values which extend more to the west over Greenland. The blocking frequency is also higher over this region under low solar activity especially between Iceland, the northern British Isles and western Scandinavia where it is significant
10 on the 95% level. The higher values extend also to the south-western part of Europe. The t850 is reduced over most of the European continent and North Africa, and higher between Greenland, the northern British Isles and Scandinavia.

3.2 Solar signal in the occurrence of the weather types

The frequencies of occurrence of CAP7 weather types for different solar activity levels for JFM are shown in Fig. 5. The size of the groups (number of months) is displayed in Table 2. The histograms display the ratios computed between the low, moderate and high solar activity frequencies and the long-term mean frequency. Histograms (a) and (b) correspond to a 123
15 and 122-year period (1763-1886 and 1887-2009). Histogram (c) (1958-2009) correspond to the reanalysis period and roughly to the period (1950-2002) analysed in (Huth et al., 2008b). Histogram (d) shows the whole period (1763-2009). For these last 50 years (c), the Northerly (N), North-Easterly (NE) and Easterly (E) types have the highest ratios under low solar activity but only the Northerly type ratio is significantly different from 1. At the same time, the West South-Westerly (WSW) and High Pressure (HP) types have the lowest ratios (significant for HP). Under high solar activity, the Easterly (E) and Northerly (N) types have a ratio lower than 1 (significant for N). Under medium activity, no ratio is significantly
20 different than 1.

For the other sub-periods of time (a) and (b) the ratios do not all show a similar signal. For example, the Northerly (N) type ratio is slightly lower than 1 for the sub-period (a) but higher than 1 for sub-period (b) under low solar activity.. This kind of
25 variability is visible in most of the weather types. Another example is the High Pressure (HP) type with a ratio significantly higher (lower) than 1 under low (moderate) solar activity in sub-period (a) but no signal in sub-period (b).. Some weather types have similar ratios in both (a) and (b). For example, under low solar activity the Westerly (W) and West South-Westerly (WSW) types ratios are lower than 1.

Although it can be difficult to deduce a general structure (similar ratios under the same solar activity level) in the weather
30 types occurrences between the different sub-periods (a), (b) and (c), there are some significant changes in the mean

occurrence of some of the types over the whole time series (1763-2009, (d)). Under low solar activity, we observe significantly lower ratios of West South-Westerly (WSW) and Westerly (W) types, and significant higher ratios of Easterly (E) type. Under moderate and high solar activity the higher Westerly (W) type ratios are significant. Under moderate solar activity the Easterly (E) and High Pressure (HP) types ratios are significantly lower than 1 as well as for the Northerly (N) type under high solar activity. Ratios computed only with days with a probability (to be correctly classified) higher than 75% (not shown), allowing us to omit some potentially erroneous weather type data, show similar results as in Fig. 5. The potential misclassified days have therefore no significant impact on our results..

The decrease in the occurrence of the Westerly type (W) is also visible with a 1, 2 and 3-year lag (Fig. 6), as for the West South-Westerly (WSW) it is only visible with a 1 year lag. The increase in the occurrence of these two types under high solar activity is visible with a 1 and 2-year lag but disappear with a 3-year lag. It is even significant for the 2-year lag. The signal found in the Northerly (N) and Easterly (E) types is inverted with a 2 and 3-year lag with a reduction in the occurrence under low solar activity. The increase in the occurrence of the High Pressure type (HP) type under low solar activity is the strongest with a 3 year lag.

The main occurrence differences for the period 1763-2009 can be summarised as follows: The occurrence of Westerly and West-South Westerly types decreases significantly under low solar activity. At the same time, we observe a significant higher occurrence of Easterly type. The occurrences of the Westerly type increases significantly under moderate and high solar activity. The occurrence of the Easterly and High Pressure (Northerly) types is significantly lower under moderate (high) solar activity.

3.3 Solar signal in weather types – within-type differences

The inter-type analysis is completed with a within-type analysis of their composites (Fig. 7 & 8). Difference composites were computed by subtracting the high from the low solar activity class composites. They were computed for the period 1958-2009 with ERA-40/-Interim and are therefore not representative of the whole 1763-2009 period. Fig. 7 displays the z500 and blocking frequency differences. Fig. 8 displays the slp and t850 differences. The weather types were originally computed with the slp over the Alpine region; thus the smallest slp differences are expected to be observed over this region. However, differences appear in the position and intensity of the high and low pressure centres, this can influence the general flow and thus the temperatures over Europe and the Alpine region.

With Fig. 7 and 8 we can identify the influence of the solar activity on each weather type and from this try to deduce a general influence on the tropospheric weather over Europe. The following descriptions always refer to the low solar activity class composite relative to the high activity one. The mean JFM weather types slp and z500 composites are shown in Fig. 3.

1 (NE): The low pressure system south of Greenland extends more to the south and less from Iceland to Scandinavia. The anticyclone is weaker over Western Europe but extends more towards Scandinavia. The low pressure system over Italy is

slightly deeper. The blocking frequency is higher from Greenland to Scandinavia but lower further south over the Atlantic. These changes in the pressure pattern lead to lower temperature over the whole European continent.

2 (WSW): The low pressure system located between Iceland and Scotland is less pronounced over Northern Europe. The mean z500 is higher between the British Isles and Scandinavia, and lower over Eastern Europe and the Mediterranean. The same pattern is visible in the temperature differences. Small differences in the blockings with higher frequencies over Scandinavia are also visible

3 (W): The pressure over Iceland is reduced whereas the Azores anticyclone is more pronounced over the Atlantic, the pressure gradient is tighter. The pressure is higher over Scandinavia and the anticyclone is more present over Southern Europe with a higher blocking frequency. Temperatures are therefore lower over most parts of Europe.

4 (E): The pressure is higher between Greenland and Scandinavia as well as the blocking frequency. The anticyclone extends more over Europe and the pressure is lower over the Mediterranean Sea. The temperature is reduced over all Europe except Scandinavia.

5 (HP): The pressure and z500 are higher over most of the North Atlantic and Northern Europe, whereas lower over Southern Europe and Northern Africa. The blocking frequency is higher over all Europe. The temperature is reduced over Europe especially in the eastern part.

6 (N): The pressure and z500 are higher over Scandinavia and lower over the Western Mediterranean Sea and Eastern Atlantic. The flow is more oriented north-easterly than north-westerly over Central Europe with reduced temperature.

7 (WC): The Azores anticyclone is more pronounced and the low pressure system between the British Isles and Scandinavia is weaker but extend more towards the Mediterranean Sea. The temperatures are reduced over South-Eastern Europe and Northern Africa, whereas warmer over North-Eastern Europe.

Similar patterns can be observed among the weather types. Types 1 (NE), 4 (E) and 6 (N) all have an enhanced easterly flow over central Europe under low solar activity and thus lower temperatures, All three types also have more frequent Scandinavian Blockings. Types 2 (WSW) and 3 (W) have a slightly reduced westerly flow over Central Europe. On average (ALL on Figs. 7 & 8, also Fig. 4) we see a higher pressure between Iceland and Scandinavia, and lower pressure over the Mediterranean Sea under low solar activity. The blocking frequency is higher between Iceland and Scandinavia too. This leads to a weaker pressure gradient and westerly flow over Europe. Following this reduction in the zonal flow, temperatures tend to be lower over Europe (except Scandinavia). Outside Europe we note an increase in temperature over the high latitude in all cases especially around Greenland.

3.4 Solar signal in model simulations

The model simulations are used to complete the analysis of the weather types and the reanalysis data. The differences between low and high solar activity obtained by four simulations (M1, M2, L1, L2) for the period 1958-1999 are displayed in Fig. 9. The low and high solar activity classes corresponds again to the 11-year solar cycle (Fig. 1). The difference plots in Fig. 9 should be comparable to Fig. 4 as well as the “ALL” plot in Fig. 7. However, none of the four simulations display a similar difference pattern as the reanalysis data. There is a lower pressure over the North Atlantic (M1), Scandinavia (L1), and Eastern Atlantic/Western Europe (L2) under low solar activity, whereas M2 shows a higher pressure and temperature over Europe. Only M1 have extended lower temperature over Europe, but the slp differences do not fit with the reanalyses data.

10 4. Discussion

The reduced zonal flow and colder temperatures over Europe under low solar activity (Fig. 4) are consistent with other studies (e.g., Brugnara et al., 2013; Ineson et al., 2011; Sfıca et al., 2015; Sirocko et al., 2012; Woollings et al., 2010). The differences over Europe resembles a more negative (positive) NAO pattern under low (high) solar activity. This kind of pattern was found in several studies (e.g., Ineson et al., 2011; Sfıca et al., 2015; Thiéblemont et al., 2015). As suggested in Thiéblemont et al. (2015) there is no direct correlation between solar activity and the NAO but a synchronisation following the downward propagation of the solar signal from the stratosphere to the troposphere. However, our results over the North Atlantic correspond more to a positive NAO under low solar activity relative to high activity with a lower slp south of Greenland and a stronger Azores high pressure system. So it seems that the 11-year cycle does not directly modulate the NAO but projects more onto west-east pattern between the Labrador Sea and Western Russia. Other studies corroborate this pattern with a solar signal extending toward Eurasia (Brugnara et al., 2013; Woollings et al., 2010). For Brugnara et al. (2013) the Eurasian index is more linked to the 11-year cycle than the NAO. The differences in the blocking index confirm the reduced zonal flow under low solar activity with a higher blocking frequency over the Norwegian Sea and Scandinavia. Similarly, Barriopedro et al. (2008) found an increase in the blocking frequency over the Eastern Atlantic under low solar activity. They also found that Atlantic blockings are located further east under low solar activity which corresponds to our result with a higher blocking frequency towards the east of the Atlantic.

The differences in weather type occurrences over the period 1958-2009 (Fig. 5 (c)) correspond well to the results of Huth et al. (2008b). It is especially the case for the West South-Westerly type with a decrease in its occurrence under low solar activity. The Northerly type shows also the same pattern as in Huth et al. (2008b) with an increase (decrease) in the occurrence under low (high) solar activity. The differences in these two types (WSW and N) are also confirmed in the long-term differences in our results (1763-2009, Fig. 5 (d)). Under low (high) solar activity the frequency of occurrence of Westerly and West-South Westerly types decreases (increases). This consecutively results in an increase in the frequency of

Easterly, High Pressure and Northerly types under low solar activity. The reduction (increase) in the occurrence of Westerly and West South-Westerly (Easterly) types is the largest difference in the ratios between one solar activity class and the long-term mean that we observe and is visible over both sub-periods (1763-1886 and 1887-2009). However, certain types (e.g. North-Easterly) do not have the same signal under both sub-periods. These types could be more sensitive to internal variability or to the influence of others forcings. As a counterexample it is interesting to see that in both sub-periods we observe a decrease in the occurrence of the Westerly type under low solar activity but it is not the case for the 1958-2009 period. This persistence of this signal over time supports the hypothesis that the 11-year solar cycle has an influence on the occurrence of European weather types.

A reduction (increase) in the occurrence of westerly types under low (high) solar activity as well as an increase in the occurrence of easterly types under low activity (Fig. 5) leads to a decrease (increase) in temperature observed in Fig. 4. These changes in the occurrence of weather types are consistent with a weaker (stronger) zonal flow over the North Atlantic and Europe, and a negative (positive) NAO-like phase pattern under low (high) solar activity as it was suggested in several studies (e.g., Ineson et al., 2011; Sfica et al., 2015).

A lagged response of the NAO following a solar maximum was suggested in Gray et al. (2013) and Thiéblemont et al. (2015). Our results with a 1 and 2-year lag (Fig. 6) showing a higher occurrence of westerly types under high solar activity also support the hypothesis of a delayed signal. However, we do not observe any signal with 3-year lag (Fig. 6 (c)) under high solar activity. Under low solar activity the weather types occurrences are similar at with no lag and a 1 year (reduction in Westerly and West South-Westerly types, slight increase in Easterly and High Pressure types). The signal found in the Northerly type with no lag is inverted with a 2 and 3-year lag (reduction in the occurrence under low solar activity). However, our results do not support previous findings suggesting that the strongest solar signal over Europe is visible with a lag.

The mesoscale circulation variations can explain the changes in the frequency of occurrence of the Easterly and Westerly weather patterns over Central Europe. A weaker zonal flow as seen in Fig. 4 leads to a reduction of the occurrences of westerly types and thus to an increase in the occurrence of easterly types (continental flow). These pattern changes are also consistent with a higher blocking index over Scandinavia under low solar activity. Blockings over high European latitudes are often responsible for the establishment of an easterly flow over Central Europe. We also observe – from 1958 to 2009 – not only a change in the weather types occurrences but also on the slp patterns of each weather type (Fig. 7 and 8). For the Westerly and West South-Westerly types we observe a reduction in the slp between Greenland and Iceland under low solar activity. Similarly to the mean difference (no weather type discrimination, Fig. 4), it resembles more to a positive NAO phase which is in contradiction with previous studies (e.g., Ineson et al., 2011; Thiéblemont et al., 2015). However, further east (toward Scandinavia) the pressure is higher under low solar activity which is synonym of a reduced oceanic flow over Central Europe and lower temperatures. So it seems that the 11-year cycle does not directly modulate the NAO but shows

more a west-east pattern between the Labrador Sea and Western Russia. As mentioned above, other studies corroborate this pattern with a solar signal extending toward Eurasia (Brugnara et al., 2013; Woollings et al., 2010).

As mentioned above, an increase in slp and blockings over Scandinavia as well as a decrease in slp over the Mediterranean Sea are synonym of an enhanced continental flow over Central Europe. We notice a double effect with an increase in the occurrence of Easterly and Northerly types (inter-type) under low solar activity but also a stronger mean easterly flow based on their composites for the period 1958-2009 (within-type). The same holds for Westerly and West South-Westerly types, which are less frequent and the associated zonal flow to these patterns is also slightly weaker over Central Europe. The stronger (weaker) continental (zonal) flow under low solar activity brings cold air from the Eurasian continent and diminishes the influence of the warm oceanic air over Central Europe. Following these circulations changes we estimate that there is a higher (lower) probability to have cold winter during the weak (strong) phase of the 11-year solar cycle. Other studies (Lockwood et al., 2010; Sirocko et al., 2012) found similar results with cold European winters being often linked to weak solar activity.

The comparison with model simulations does not confirm our observation-based results on the mean slp over the North Atlantic and Europe. The response of the slp and t850 to the 11-year solar cycle does not display any clear pattern, each simulation having a different response. Although the model is forced with six bands of SSI, there is no agreement in-between the four simulations on a solar signal on the surface pressure over Europe. The low amplitude of the 11-year cycle in the Shapiro reconstruction (compared to the large amplitude of the low frequency activity) combined with the relatively coarse resolution of the model could explain the difficulty of the model to capture changes over a specific region.

5. Conclusion

We have used a new weather types classification to analyse the impact of the 11-year solar cycle on European weather in late winter. The monthly sunspot number was used as a measure of solar activity and the daily weather types were retrieved from the CAP7 classification. We have analysed changes in the frequency of occurrence of the CAP7 weather types under three different solar activity levels (low, moderate, high) from 1763 to 2009 and analysed as well the within-type differences between low and high solar activity from 1958 to 2009 in reanalyses data. The mean difference in the sea level pressure and 850 hPa temperature was then compared with four model simulations.

The strongest solar signal visible in the occurrence of the CAP7 weather types is a reduction in the number of days with westerly and west south-westerly flow under low solar activity. Consequently, in the number of days with a northerly, easterly flow and high pressure increases. Conversely, the occurrence of both westerly and west south-westerly types increases under moderate and high solar activity. The analysis of within-type differences under low and high solar activity phases confirms that not only the frequency of occurrence of some weather types respond to change in the solar activity, but also the mean patterns of these types are slightly different. The zonal flow characteristic of westerly types is reduced under

low solar activity as the continental flow for easterly and northerly types is enhanced. This is also confirmed by the higher blocking frequency over Scandinavia under low solar activity. The sea level pressure differences observed in the reanalysis data are not supported by the SOCOL-MPIOM model simulations. The coarse resolution of the model is not suited for an analysis of the 11-year solar cycle impact on tropospheric weather.

5 The 247-year long analysis of the 11-year solar cycle impact on late winter European weather patterns suggest a reduction in the occurrence of westerly flow types linked to a reduced mean zonal flow under low solar activity. Following these observation, we estimate the probability to have cold conditions in winter over Europe to be higher under low solar activity than under high activity.

10 **Acknowledgments.** This work was funded by the Swiss National Science Foundation through the Sinergia FUPSOL II (Number 147659). We thank ECMWF for providing ERA-40 and ERA-Interim data. We also thank the World Data Center (WDX-SILSO, Royal Observatory of Belgium, Brussels) for the production, preservation and dissemination of the international Sunspot Number.

References

15 Andersson, M. E., Verronen, P. T., Rodger, C. J., Clilverd, M. A. and Seppälä, A.: Missing driver in the Sun-Earth connection from energetic electron precipitation impacts mesospheric ozone., *Nat. Commun.*, 5(May), 5197, doi:10.1038/ncomms6197, 2014.

Arfeuille, F., Weisenstein, D., MacK, H., Rozanov, E., Peter, T. and Brönnimann, S.: Volcanic forcing for climate modeling: 20 A new microphysics-based data set covering years 1600-present, *Clim. Past*, 10(1), 359–375, doi:10.5194/cp-10-359-2014, 2014.

Barriopedro, D., García-Herrera, R. and Huth, R.: Solar modulation of Northern Hemisphere winter blocking, *J. Geophys. Res. Atmos.*, 113(14), 1–11, doi:10.1029/2008JD009789, 2008.

25

Brugnara, Y., Brönnimann, S., Luterbacher, J. and Rozanov, E.: Influence of the sunspot cycle on the Northern Hemisphere wintertime circulation from long upper-air data sets, *Atmos. Chem. Phys.*, 13(13), 6275–6288, doi:10.5194/acp-13-6275-2013, 2013.

30 Dee, D. P., Uppala, S. M., Simmons, A. J., Berrisford, P., Poli, P., Kobayashi, S., Andrae, U., Balmaseda, M. A., Balsamo, G., Bauer, P., Bechtold, P., Beljaars, A. C. M., van de Berg, L., Bidlot, J., Bormann, N., Delsol, C., Dragani, R., Fuentes, M.,

- Geer, A. J., Haimberger, L., Healy, S. B., Hersbach, H., Hólm, E. V., Isaksen, I., Kållberg, P., Köhler, M., Matricardi, M., McNally, A. P., Monge-Sanz, B. M., Morcrette, J. J., Park, B. K., Peubey, C., de Rosnay, P., Tavolato, C., Thépaut, J. N. and Vitart, F.: The ERA-Interim reanalysis: Configuration and performance of the data assimilation system, *Q. J. R. Meteorol. Soc.*, 137(656), 553–597, doi:10.1002/qj.828, 2011.
- 5
- Etheridge, D., Steele, L., Langenfelds, R., Francey, R., Barnola, J., and Morgan, V.: Natural and anthropogenic changes in atmospheric CO₂ over the last 1000 years from air in Antarctic ice and firn, *J. Geophys. Res.*, 101, 4115–4128, doi:10.1029/95JD03410, 1996.
- 10
- Etheridge, D. M., Steele, L. P., Francey, R. J., and Langenfelds, R. L.: Atmospheric methane between 1000 A.D. and present: Evidence of anthropogenic emissions and climatic variability, *J. Geophys. Res.*, 103, 15979–15993, doi:10.1029/98JD00923, 1998.
- Ferretti, D. F., Miller, J. B., White, J. W. C., Etheridge, D. M., Lassey, K. R., Lowe, D. C., Meure, C. M. M. F., Dreier, M.
- 15
- F., Trudinger, C. M., Van Ommen, T. D., and Langenfelds, R. L.: Unexpected changes to the global methane budget over the past 2000 years, *Science*, 309, 1714–1717, doi:10.1126/science.1115193, 2005.
- Gimeno, L., de la Torre, L., Nieto, R., García, R., Hernández, E. and Ribera, P.: Changes in the relationship NAO-Northern hemisphere temperature due to solar activity, *Earth Planet. Sci. Lett.*, 206(1–2), 15–20, doi:10.1016/S0012-821X(02)01090-7, 2003.
- 20
- Gray, L. J., Beer, J., Geller, M., Haigh, J. D., Lockwood, M., Matthes, K., Cubasch, U., Fleitmann, D., Harrison, G., Hood, L., Luterbacher, J., Meehl, G. a., Shindell, D., van Geel, B. and White, W.: Solar influence on climate, *Rev. Geophys.*, 48(2009), RG4001, doi:10.1029/2009RG000282, 2010.
- 25
- Gray, L. J., Scaife, A. A., Mitchell, D. M., Osprey, S., Ineson, S., Hardiman, S., Butchart, N., Knight, J., Sutton, R. and Kodera, K.: A lagged response to the 11 year solar cycle in observed winter Atlantic/European weather patterns, *J. Geophys. Res. Atmos.*, 118(24), 13405–13420, doi:10.1002/2013JD020062, 2013.
- 30
- Hood, L. L., Misios, S., Mitchell, D. M., Rozanov, E., Gray, L. J., Tourpali, K., Matthes, K., Schmidt, H., Chiodo, G., Thiéblemont, R., Shindell, D. and Krivolutsky, A.: Solar signals in CMIP-5 simulations: The ozone response, *Q. J. R. Meteorol. Soc.*, 141(692), 2670–2689, doi:10.1002/qj.2553, 2015.
- Huth, R., Bochníček, J. and Hejda, P.: The 11-year solar cycle affects the intensity and annularity of the Arctic Oscillation, *J.*

Atmos. Solar-Terrestrial Phys., 69(9), 1095–1109, doi:10.1016/j.jastp.2007.03.006, 2007.

5 Huth, R., Beck, C., Philipp, A., Demuzere, M., Ustrnul, Z., Cahynová, M., Kyselý, J. and Tveito, O. E.: Classifications of atmospheric circulation patterns: Recent advances and applications, *Ann. N. Y. Acad. Sci.*, 1146, 105–152, doi:10.1196/annals.1446.019, 2008a.

Huth, R., Kyselý, J., Bochníček, J. and Hejda, P.: Solar activity affects the occurrence of synoptic types over Europe, *Ann. Geophys.*, 26, 1999–2004, 2008b.

10 Ineson, S., Scaife, A. a., Knight, J. R., Manners, J. C., Dunstone, N. J., Gray, L. J. and Haigh, J. D.: Solar forcing of winter climate variability in the Northern Hemisphere, *Nat. Geosci.*, 4(11), 753–757, doi:10.1038/ngeo1282, 2011.

Lockwood, M.: Solar Influence on Global and Regional Climates, *Surv. Geophys.*, 33(3–4), 503–534, doi:10.1007/s10712-012-9181-3, 2012.

15

Lockwood, M., Harrison, R. G., Woollings, T. and Solanki, S. K.: Are cold winters in Europe associated with low solar activity?, *Environ. Res. Lett.*, 5(2), 24001, doi:10.1088/1748-9326/5/2/024001, 2010.

20 Van Loon, H. and Meehl, G. A.: Interactions between externally forced climate signals from sunspot peaks and the internally generated Pacific Decadal and North Atlantic Oscillations, *Geophys. Res. Lett.*, 41(1), 161–166, doi:10.1002/2013GL058670, 2014.

25 MacFarling-Meure, C., Etheridge, D., Trudinger, C., Steele, P., Langenfelds, R., Van Ommen, T., Smith, A., and Elkins, J.: Law Dome CO₂, CH₄ and N₂O ice core records extended to 2000 years BP, *Geophys. Res. Lett.*, 33, L14810, doi:10.1029/2006GL026152, 2006.

Martin-Puertas, C., Matthes, K., Brauer, A., Muscheler, R., Hansen, F., Petrick, C., Aldahan, A., Possnert, G. and van Geel, B.: Regional atmospheric circulation shifts induced by a grand solar minimum, *Nat. Geosci.*, 5(6), 397–401, doi:10.1038/ngeo1460, 2012.

30

Matthes, K., Kodera, K., Haigh, J. D., Shindell, D. T., Shibata, K., Langematz, U., Rozanov, E. and Kuroda, Y.: GRIPS Solar Experiments Intercomparison Project: Initial results, *Pap. Meteorol. Geophys.*, 54(2), 71–90, doi:10.2467/mripapers.54.71, 2003.

- Matthes, K., Langematz, U., Gray, L. J., Kodera, K. and Labitzke, K.: Improved 11-year solar signal in the free university of Berlin climate middle atmosphere model (FUB-CMAM), *J. Geophys. Res.*, 109, 1–15, doi:10.1029/2003JD004012, 2004.
- Misios, S., Mitchell, D. M., Gray, L. J., Tourpali, K., Matthes, K., Hood, L., Schmidt, H., Chiodo, G., Thieblemont, R.,
5 Rozanov, E. and Krivolutsky, A.: Solar signals in CMIP-5 simulations: Effects of atmosphere-ocean coupling, *Q. J. R. Meteorol. Soc.*, 142(695), 928–941, doi:10.1002/qj.2695, 2016.
- Mitchell, D. M., Misios, S., Gray, L. J., Tourpali, K., Matthes, K., Hood, L., Schmidt, H., Chiodo, G., Thieblemont, R.,
10 Rozanov, E., Shindell, D. and Krivolutsky, A.: Solar signals in CMIP-5 simulations: the stratospheric pathway, *Q. J. R. Meteorol. Soc.*, 141, 2390–2403, doi:10.1002/qj.2530, 2015.
- Moffa-Sánchez, P., Born, A., Hall, I. R., Thornalley, D. J. R. and Barker, S.: Solar forcing of North Atlantic surface temperature and salinity over the past millennium, *Nat. Geosci.*, 7(April), 275–278, doi:10.1038/NGEO2094, 2014.
- 15 Muthers, S., Anet, J. G., Stenke, A., Raible, C. C., Rozanov, E., Brönnimann, S., Peter, T., Arfeuille, F. X., Shapiro, A. I., Beer, J., Steinhilber, F., Brugnara, Y. and Schmutz, W.: The coupled atmosphere-chemistry-ocean model SOCOL-MPIOM, *Geosci. Model Dev.*, 7(5), 2157–2179, doi:10.5194/gmd-7-2157-2014, 2014.
- Oldenborgh, G. J. Van, Laats, T. J. De, Luterbacher, J., Ingram, W. J. and Osborn, T. J.: Claim of solar influence is on thin
20 ice: are 11-year cycle solar minima associated with severe winters in Europe?, *Environ. Res. Lett.*, 8(2), 24014, doi:10.1088/1748-9326/8/2/024014, 2013.
- Päivärinta, S. M., Seppälä, A., Andersson, M. E., Verronen, P. T., Thölix, L. and Kyrölä, E.: Observed effects of solar proton events and sudden stratospheric warmings on odd nitrogen and ozone in the polar middle atmosphere, *J. Geophys. Res.*
25 *Atmos.*, 118(12), 6837–6848, doi:10.1002/jgrd.50486, 2013.
- Philipp, A., Bartholy, J., Beck, C., Erpicum, M., Esteban, P., Fettweis, X., Huth, R., James, P., Jourdain, S., Kreienkamp, F., Krennert, T., Lykoudis, S., Michalides, S. C., Pianko-Kluczynska, K., Post, P., Álvarez, D. R., Schiemann, R., Spekat, A. and Tymvios, F. S.: Cost733cat - A database of weather and circulation type classifications, *Phys. Chem. Earth*, 35(9–12),
30 360–373, doi:10.1016/j.pce.2009.12.010, 2010.
- Philipp, A., Beck, C., Huth, R. and Jacobbeit, J.: Development and comparison of circulation type classifications using the COST 733 dataset and software, *Int. J. Climatol.*, 36(7), 2673–2691, doi:10.1002/joc.3920, 2014.

- Robock, A.: Volcanic eruptions and climate, , 38(2), 191–219, doi:10.1029/1998RG000054, 2000.
- Rozañov, E., Calisto, M., Egorova, T., Peter, T. and Schmutz, W.: Influence of the Precipitating Energetic Particles on Atmospheric Chemistry and Climate, *Surv. Geophys.*, 33(3–4), 483–501, doi:10.1007/s10712-012-9192-0, 2012.
- 5 Scherrer, S. C., Croci-Maspoli, M., Schwierz, C. and Appenzeller, C.: Two-dimensional indices of atmospheric blocking and their statistical relationship with winter climate patterns in the Euro-Atlantic region, *Int. J. Climatol.*, 26(2), 233–249, doi:10.1002/joc.1250, 2006.
- 10 Schwander, M., Bröñnimann, S., Delaygue, G., Rohrer, M., Auchmann, R. and Brugnara, Y.: Reconstruction of Central European daily weather types back to 1763, *Int. J. Climatol.*, doi:10.1002/joc.4974, 2017.
- Seppälä, A., Matthes, K., Randall, C. E. and Mironova, I. a: What is the solar influence on climate? Overview of activities during CAWSES-II, *Prog. Earth Planet. Sci.*, 1(1), 24, doi:10.1186/s40645-014-0024-3, 2014.
- 15 Sfıca, L., Voiculescu, M. and Huth, R.: The influence of solar activity on action centres of atmospheric circulation in North Atlantic, *Ann. Geophys.*, 33(2), 207–215, doi:10.5194/angeo-33-207-2015, 2015.
- Sirocko, F., Brunck, H. and Pfahl, S.: Solar influence on winter severity in central Europe, *Geophys. Res. Lett.*, 39(16), 2–6, doi:10.1029/2012GL052412, 2012.
- 20 Sitnov, S. A.: Influence of the 11-year solar cycle on the effects of the equatorial quasi-biennial oscillation, manifesting in the extratropical northern atmosphere, *Clim. Dyn.*, 32(1), 1–17, doi:10.1007/s00382-007-0362-6, 2009.
- 25 Solomon, S., Crutzen, P. J. and Roble, R. G.: Photochemical coupling between the thermosphere and the lower atmosphere: 1. Odd nitrogen from 50 to 120 km, *J. Geophys. Res.*, 87, 7206, doi:10.1029/JC087iC09p07206, 1982.
- Stevens, M. J. and North, G. R.: Detection of the climate response to the solar cycle, *J. Atmos. Sci.*, 53(18), 2594–2608, doi:10.1175/1520-0469(1996)053<2594:DOTCRT>2.0.CO;2, 1996.
- 30 Thiéblemont, R., Matthes, K., Omrani, N.-E., Kodera, K. and Hansen, F.: Solar forcing synchronizes decadal North Atlantic climate variability, *Nat. Commun.*, 6, 8268, doi:10.1038/ncomms9268, 2015.
- Tibaldi, S. and Molteni, F.: On the operational predictability of blocking, *Tellus A*, 42(3), 343–365, doi:10.1034/j.1600-

Uppala, S. M., Kallberg, P. W., Simmons, A. J., Andrae, U., Bechtold, V. D., Fiorino, M., Gibson, J. K., Haseler, J., Hernandez, A., Kelly, G. A., Li, X., Onogi, K., Saarinen, S., Sokka, N., Allan, R. P., Andersson, E., Arpe, K., Balmaseda, M.
5 A., Beljaars, A. C. M., Van De Berg, L., Bidlot, J., Bormann, N., Caires, S., Chevallier, F., Dethof, A., Dragosavac, M., Fisher, M., Fuentes, M., Hagemann, S., Holm, E., Hoskins, B. J., Isaksen, L., Janssen, P. A. E. M., Jenne, R., McNally, A. P., Mahfouf, J. F., Morcrette, J. J., Rayner, N. A., Saunders, R. W., Simon, P., Sterl, A., Trenberth, K. E., Untch, A., Vasiljevic, D., Viterbo, P. and Woollen, J.: The ERA-40 re-analysis, *Q. J. R. Meteorol. Soc.*, 131(612), 2961–3012, doi:10.1256/qj.04.176, 2005.

10

Weusthoff, T.: Weather Type Classification at MeteoSwiss - Introduction of new automatic classification schemes, *Arbeitsberichte der MeteoSchweiz*, (235), 46, 2011.

White, W. B., Lean, J., Cayan, D. R. and Dettinger, M. D.: Response of global upper ocean temperature to changing solar
15 irradiance, *J. Geophys. Res.*, 102(C2), 3255–3266, doi:10.1029/96JC03549, 1997.

Woollings, T., Lockwood, M., Masato, G., Bell, C. and Gray, L.: Enhanced signature of solar variability in Eurasian winter climate, *Geophys. Res. Lett.*, 37(20), 1–6, doi:10.1029/2010GL044601, 2010.

20

Table 1: CAP7 weather types numbers, abbreviations and names

Index	Abbreviation	Full Name
1.	NE	North-East, indifferent
2.	WSW	West South-West, cyclonic, flat pressure
3.	W	Westerly flow over Northern Europe
4.	E	East, indifferent
5.	HP	High Pressure over Europe
6.	N	North, cyclonic
7.	WC	Westerly flow over Southern Europe, cyclonic

Table 2: Size (number of months) of each solar activity level and periods analysed

	1763-1886	1887-2009	1958-2009	1763-2009
low	98	99	38	195
moderate	108	102	35	211
high	106	105	47	212

5

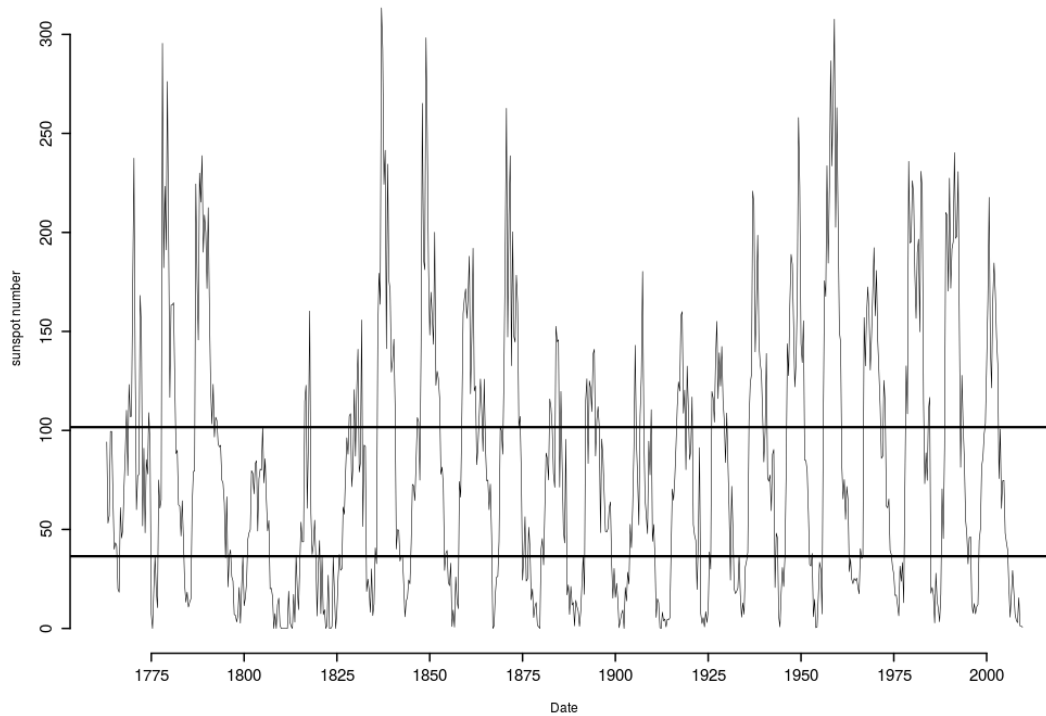


Figure 1: 1763-2009 JFM monthly sunspot number with 33rd and 66th percentile thresholds.

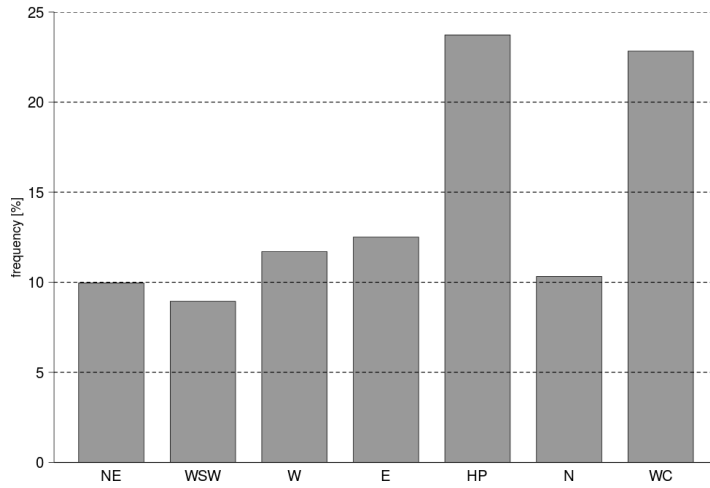
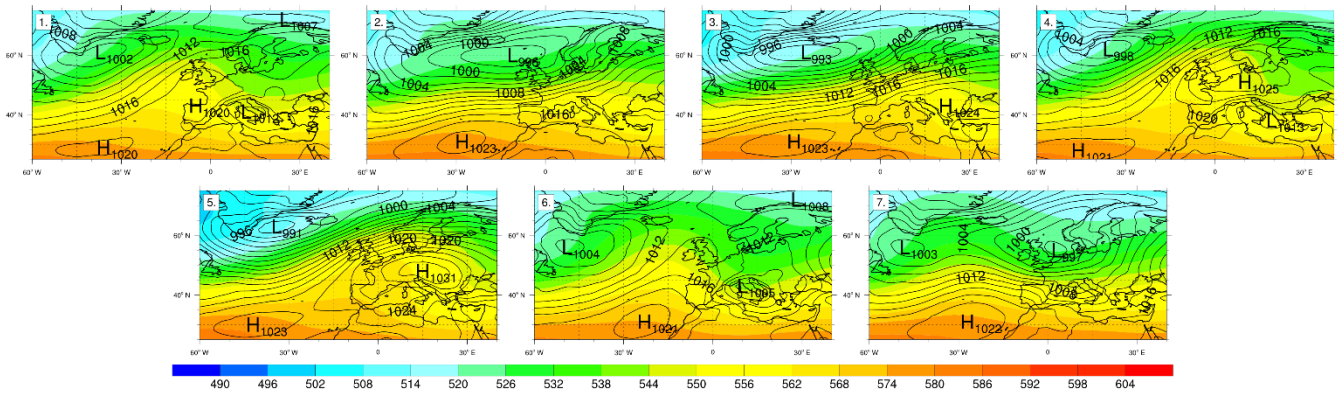


Figure 2: CAP7 1763-2009 JFM mean frequency of occurrence.



5 Figure 3: CAP7 1958-2009 500 hPa geopotential height (color) and sea level pressure (contours) JFM composites.

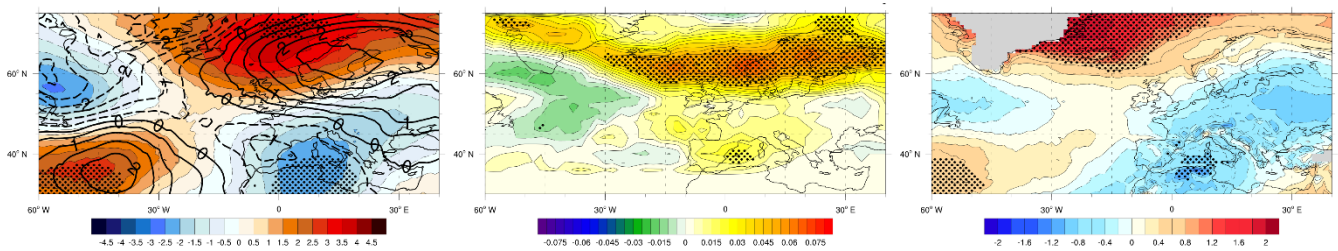


Figure 4: 1958-2009 low minus high solar activity differences computed with ERA-40/Interim. Left: 500 hPa geopotential height (color) and sea level pressure (contour). Centre: blocking frequency. Right 850 hPa temperature. The 95% significance level is indicated with stippled areas.

10

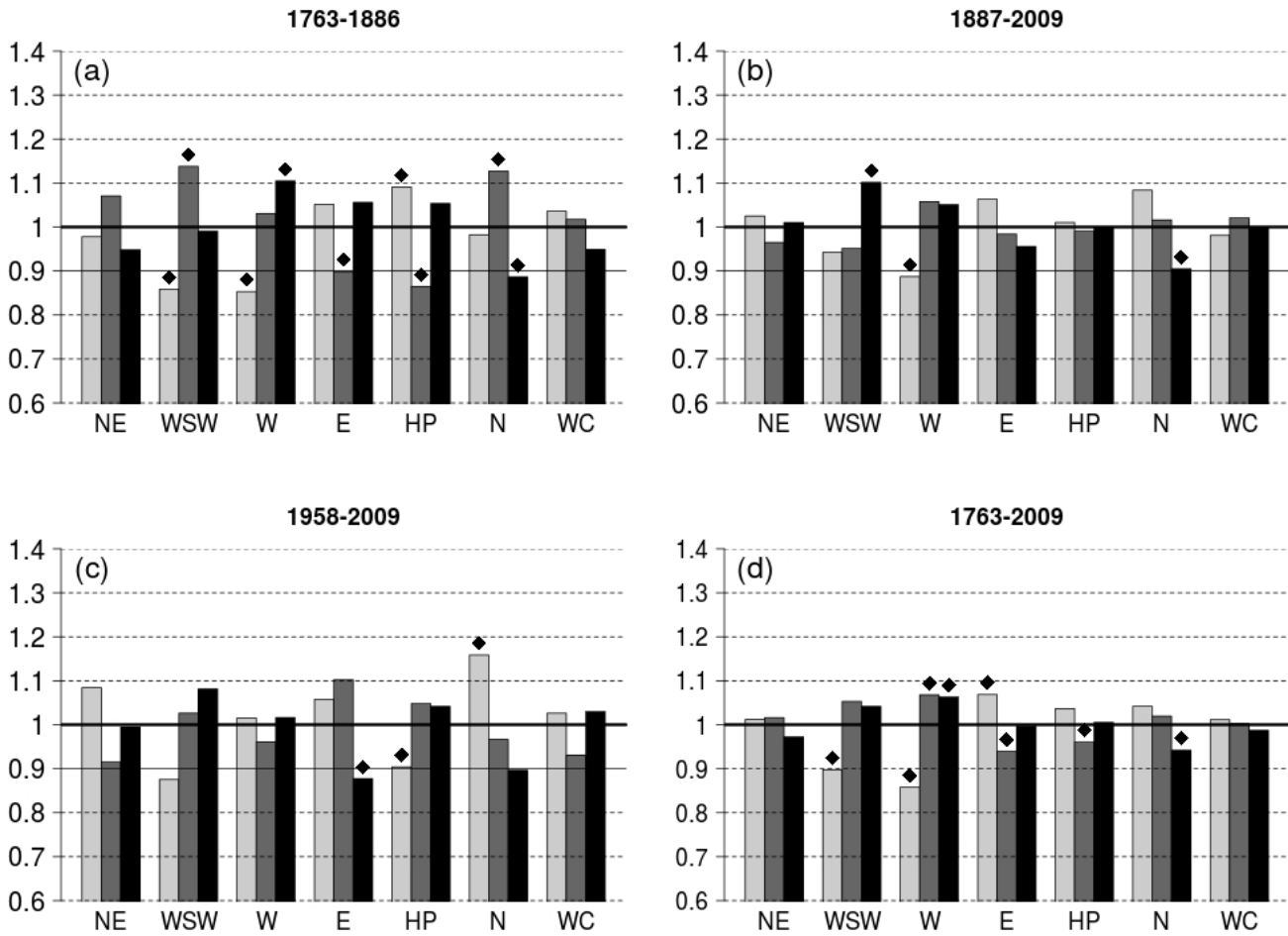


Figure 5: Ratios of the frequency for the low (light grey), moderate (grey) and high (black) solar activity classes for different periods. Dots correspond to statistical significance of the ratios at the 95% level.

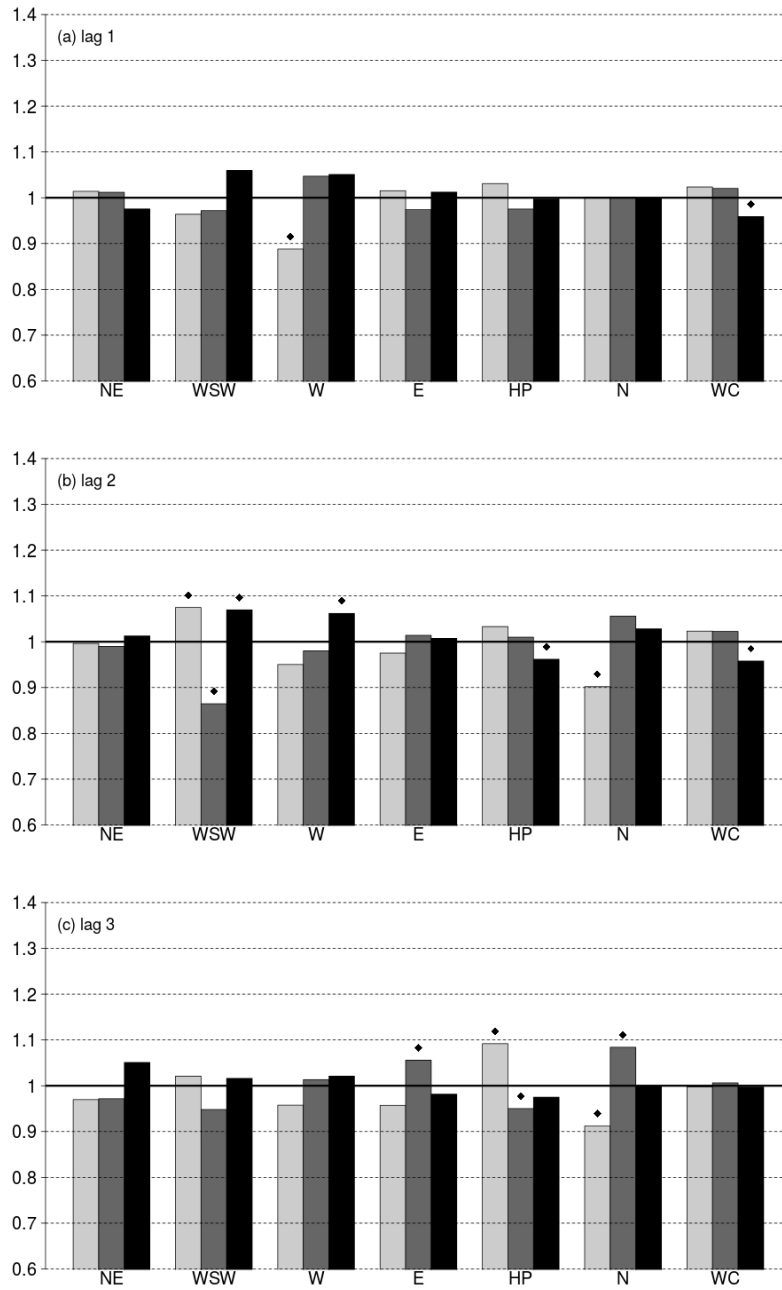


Figure 6: Ratios of the frequency for the low (light grey), moderate (grey) and high (black) solar activity classes for 1 (a), 2 (b) and 3 (c) years lags. Dots correspond to statistical significance of the ratios at the 95% level.

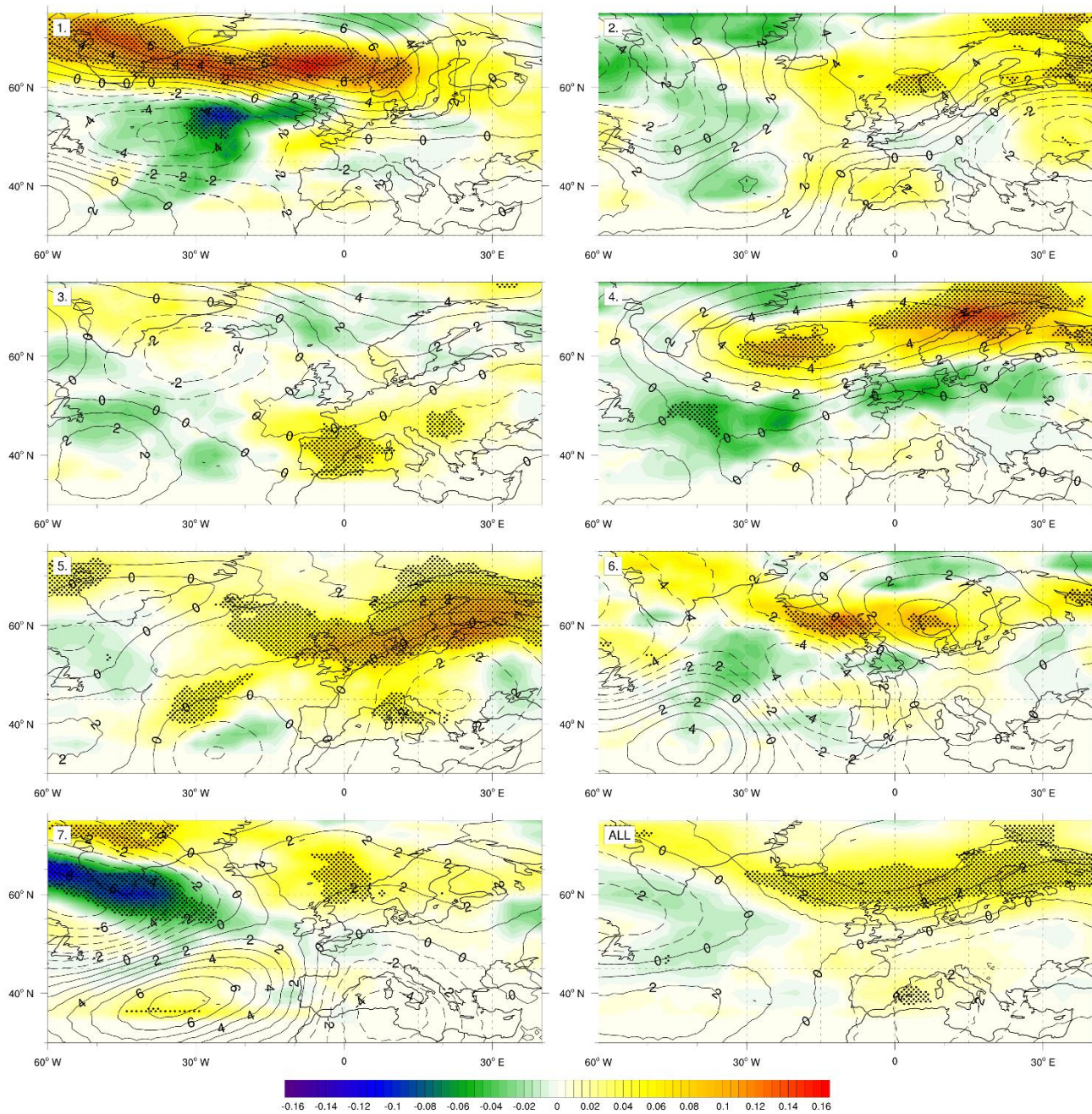


Figure 7: CAP7 (1 to 7) and mean (ALL) JFM blocking frequency (color) and 500 hPa geopotential height (contour) difference between low and high solar activity (low minus high) computed with ERA-40/-Interim for 1958-2009. The 95% significance level is indicated with stippled areas.

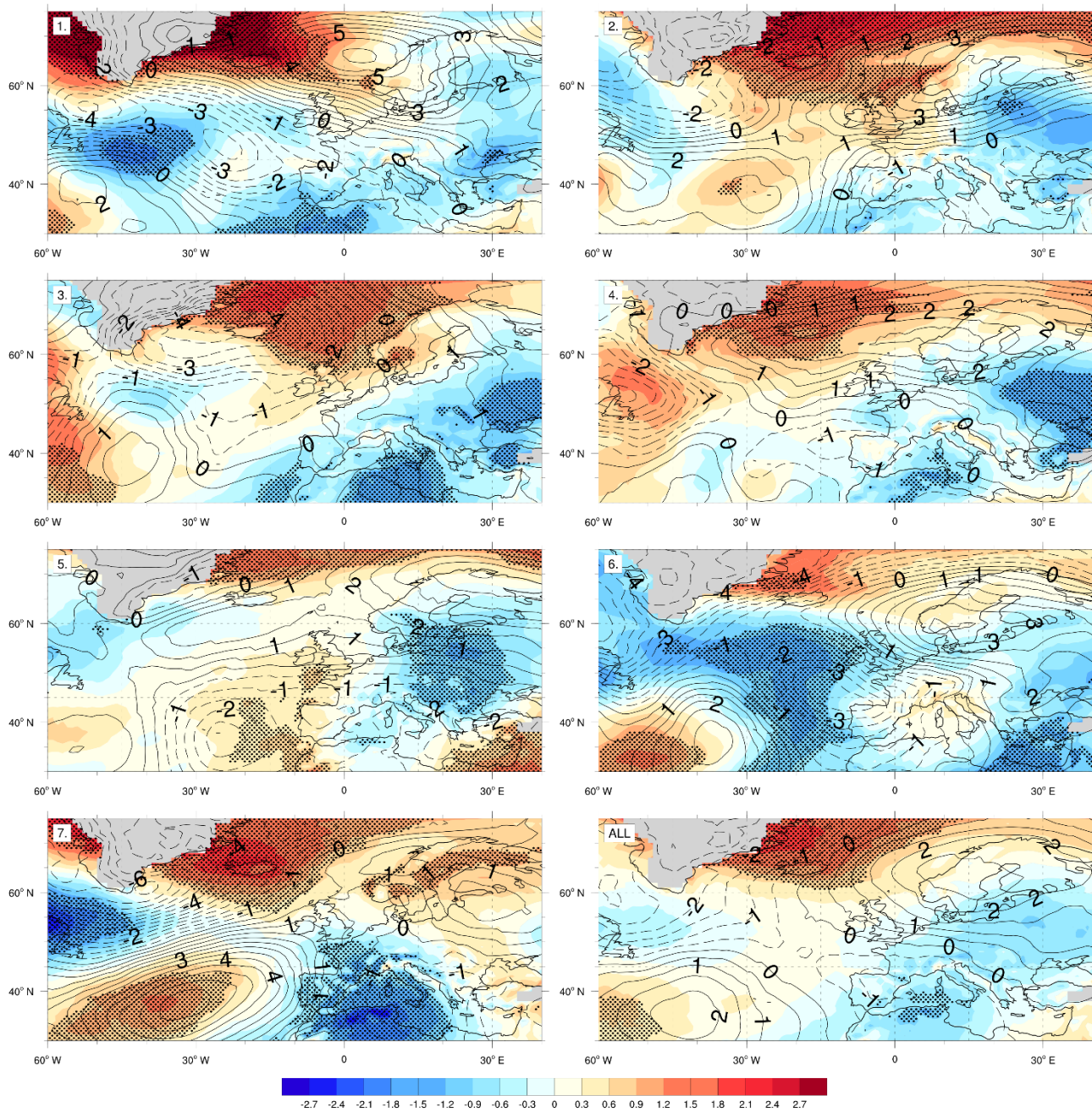


Figure 8: CAP7 (1 to 7) and mean (ALL) JFM sea level pressure (contour) and 850 hPa temperature (colour) difference between low and high solar activity (low minus high) computed with ERA-40/Interim for 1958-2009. The 95% significance level is indicated with stippled areas.

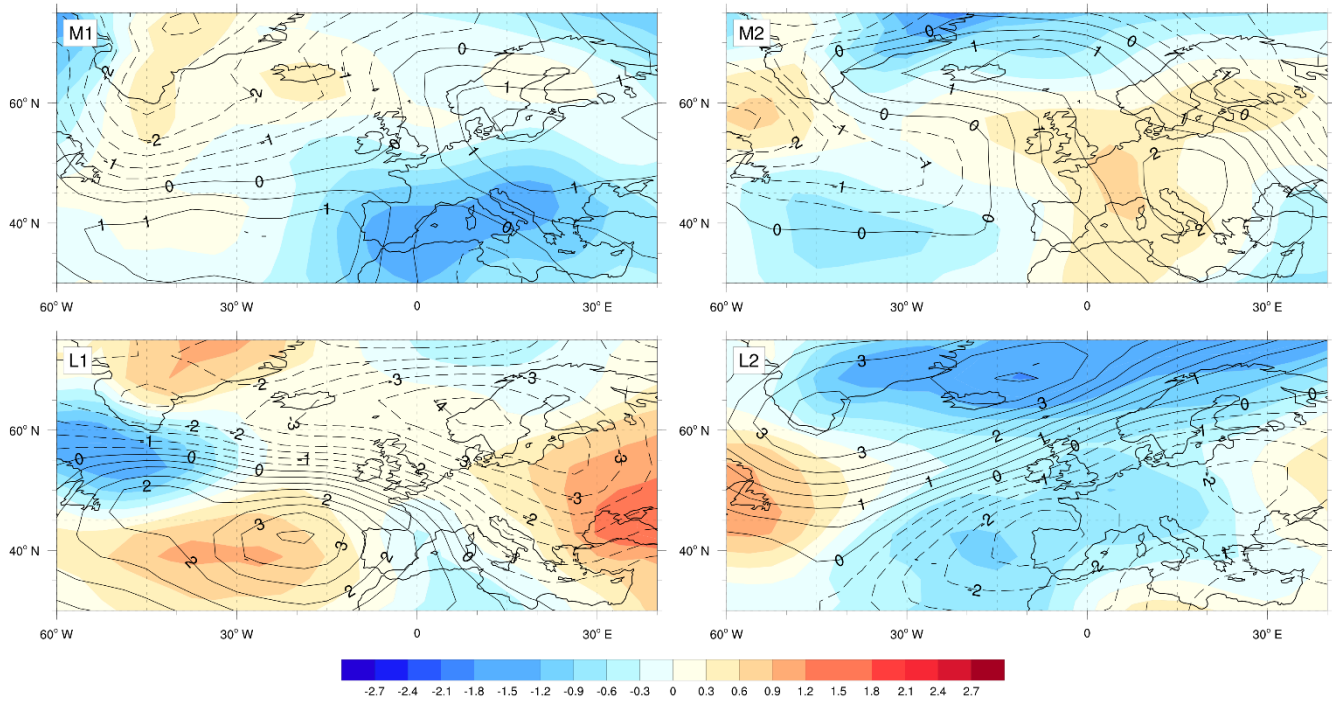


Figure 9: JFM sea level pressure (contour) and 850 hPa temperature (colour) difference between 11-year cycle low and high solar activity (high frequency) computed with the model simulations for 1958-1999.